JOURNAL OF MATERIALS SCIENCE **36** (2001) 2349–2357

Two-phase porous silica: Mesopores inside controlled pore glasses

D. ENKE, K. OTTO, F. JANOWSKI, W. HEYER
Institute of Technical Chemistry and Macromolecular Chemistry, Martin-Luther-University Halle-Wittenberg, Schloßberg 2, D-06108 Halle/Saale, Germany

W. SCHWIEGER
Institute of Technical Chemistry I, University Erlangen-Nürnberg, Egerlandstraße 3, D-91058 Erlangen, Germany

W. GILLE
Department of Physics, Martin-Luther-University Halle-Wittenberg, SAS-Laboratory, Hoher Weg 8, D-06120 Halle/Saale, Germany

The structural and textural properties of "Two-Phase Porous Silica" consisting of a mesoporous pore system formed by finely dispersed silica-gel inside the original pores of a macroporous glass framework have been carefully investigated. Nitrogen adsorption at 77 K, Mercury Intrusion, Small Angle X-ray Scattering (SAXS), Temperature-Programmed Desorption (TPD) of ammonia and ^{27}Al MAS NMR spectroscopy were used. Different mesoporous glasses investigated show BET surface areas up to 300 m^2/g, a total pore volume of about 0.16 cm^3/g and pore sizes of $<$2–10 nm, depending on the acid leaching conditions of the phase-separated sodium borosilicate initial glass. The texture of the macroporous "frame" glass was characterized after removing the mesoporous finely dispersed silica-gel phase with alkaline solution. Leaching of the phase-separated initial glass with $Al(NO_3)_3$ solution and followed by thermal treatment lead to the formation of Brönsted acid sites at the surface of the resulting mesoporous glasses by an incorporation of aluminium in tetrahedral coordination in the silica framework.

1. Introduction

Increasing research in the fields of chemical sensors [1], membrane science [2], micro-reaction engineering, biotechnology and confined matter [3] has evoked a renaissance in the use of Controlled Pore Glass (CPG), especially with mesopores, lying in the range between 2 and 50 nm. CPG's, in comparison with other porous inorganic solids, possess several advantages, for example a tailorable pore size between 0.3 and 1000 nm, large specific surface areas, high thermal stability and high resistance to acids. They can be prepared in various geometric forms, i.e., as beads, rods and plates. Some important commercial applications of CPG's are found in biochemistry as matrix for enzyme immobilization [4] and as packing material for HPLC [5].

Since the early fourties Porous VYCOR Glass (PVG) has been prepared by phase-separation of alkali borosilicate glasses followed by acid leaching [6, 7]. At first, a heat-treatment leads to phase-separation of the alkali borosilicate glasses. Two different phases are obtained, the first one being almost pure silica. The second one is an alkali-rich borate phase with certain amounts of silica dissolved in it [8, 9]. After acid leaching, due to the very low solubility of silica in acidic medium, SiO_2-aggregates remain as finely dispersed silica-gel in the cavities of the main silica framework of the macroporous glasses. The finely dispersed silica-gel affects the pore structure and the properties of the resulting porous glass system [10]. This effect is exploited for the preparation of the so-called Controlled Pore Glass (CPG) [11].

The finely dispersed silica-gel increases the specific surface area of the material. However, the specific pore volume and the mass transport through the porous glass are reduced. Usually the finely dispersed silica-gel is precipitated on the pore walls of the CPG's respectively only fills parts of the porous glass framework. This effect is unwished for most applications of CPG's. Therefore, the finely dispersed silica-gel has been removed by treatment with alkaline solution [11]. However, in some special applications it can be very useful, for example, as membranes for gas separation, in the preparation of new bisilicate composite materials (zeolite/CPG) or in micro-reaction engineering.

This paper describes the preparation and characterization of "Two-Phase Porous Silica" consisting of a macroporous framework and a mesoporous pore system formed by the finely dispersed silica-gel inside the

original macropores of the porous glass. In particular, the textural and structural properties of the mesoporous silica-gel phase have been investigated.

2. Experimental

A spherical sodium borosilicate initial glass (70 wt.-% SiO_2, 23 wt.-% B_2O_3, 7 wt.-% Na_2O), 0.3–0.5 mm in diameter (Fig. 1) was phase-separated at 630°C for 24 hours.

The formation of the mesoporous phases inside the macroporous "frame"-glasses was initiated by various acid leaching conditions of the phase-separated initial glass resulting in the claimed mesoporous "Two-Phase Porous Silica" (MePG), schematically shown in Table I. The ratio of the volume of leaching acid (HCl, $Al(NO_3)_3$) to the weight of phase-separated initial glass (ml solution/g glass) was maintained at a constant value of 15. In the case of leaching the initial glass with aluminium nitrate solution, the resulting mesoporous "Two-Phase Porous Silica" (MePG 5/1.0, MePG 6/0.7) were calcined at 550 and 700°C to consolidate surface and microstructure.

TABLE I Preparation of the porous glasses

Sample	Preparation	wt.-% Al_2O_3 (ICP)
MePG 1	Leaching 3 N HCl 30 min 90°C	-
MePG 2	Leaching 3 N HCl 10 h 90°C	-
MePG 3	Leaching 6 N HCl 10 h 90°C	-
MePG 4	Leaching 3 N HCl 40 h 90°C	-
MePG 5/1.0	Leaching 3 M $Al(NO_3)_3$ 40 h 90°C Calcination 5 h 550°C	1.0
MePG 6/0.7	Leaching 3 M $Al(NO_3)_3$ 40 h 90°C Calcination 5 h 700°C	0.7
MaPG	Treatment sample MePG 2 0.5 N NaOH 2 h RT Calcination 2 h 700°C Leaching 3 N HCl 10 h 90°C	-

In order to uncover the properties of the "frame"-glass (MaPG) an alkaline leaching, a calcination and an additional acid leaching have to be carried out to remove the finely dispersed silica-gel completely from the macropores in the CPG. This removal is proved by results of the Mercury Intrusion experiments.

The adsorption properties of the samples were characterized using nitrogen adsorption at 77 K. First, all samples were degassed at 120°C for 8 h. Adsorption and desorption isotherms were measured over a range of relative pressures (P/P_0) from 0 to 1.0 for all mesoporous glasses on a Sorptomatic 1900 apparatus by Carlo Erba Instruments.

Surface areas were determined from the linear form of the BRUNAUER-EMMETT-TELLER (BET) equation in a relative pressure range (P/P_0) of the adsorption isotherms between 0.05 and 0.25 [12]. A value of 0.162 nm^2 was used for the cross-sectional area of one nitrogen molecule. The total pore volume V_P was estimated from the amount of vapour adsorbed at the relative pressure $P/P_0 = 0.99$ assuming that pores are filled subsequently with condensed adsorptive in the normal liquid state. The pore size distributions of the mesoporous glasses were determined from the adsorption and desorption branches of the nitrogen sorption

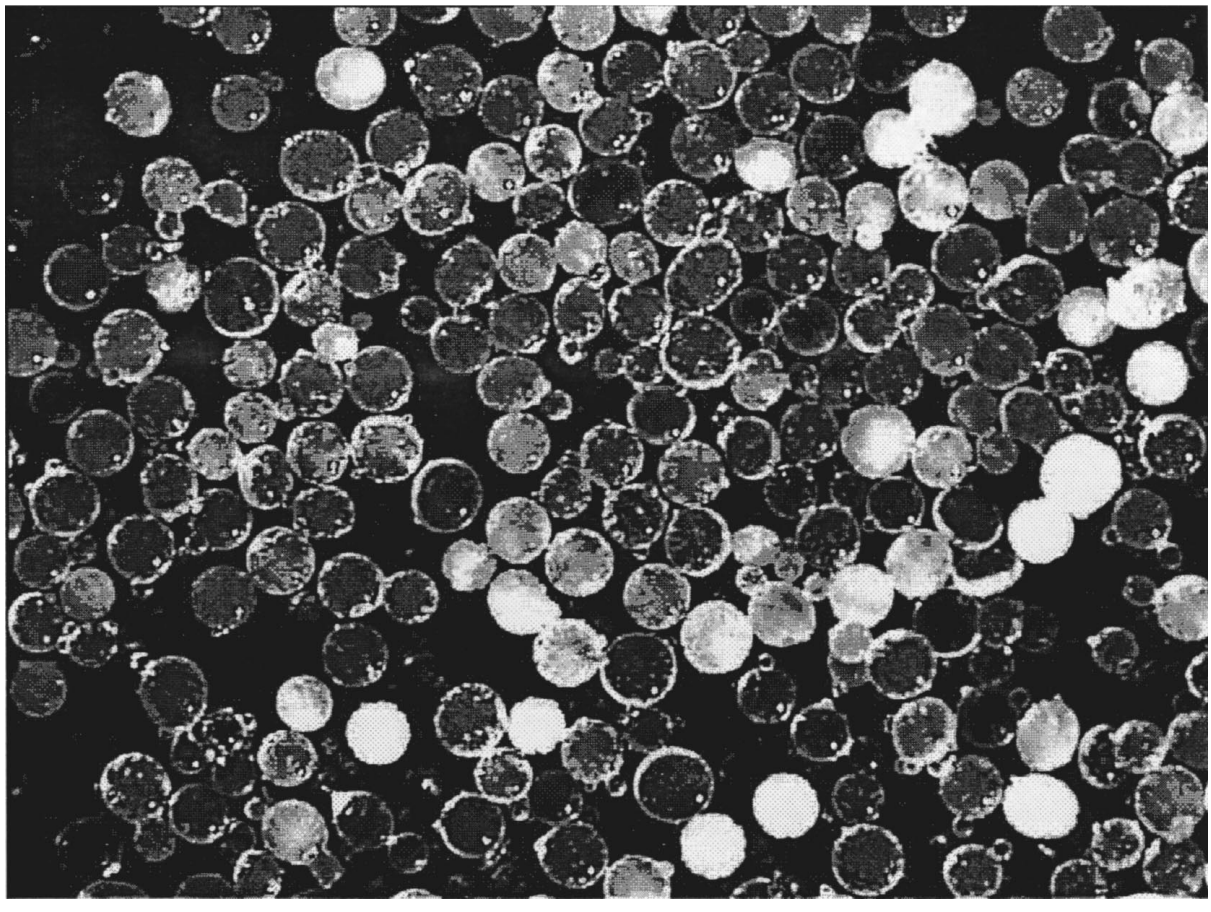

Figure 1 Glass beads (0.3–0.5 mm in diameter).

isotherm according to the BJH (Barret, Joyner, and Halenda) method, based on the Kelvin equation, which relates the pore size with critical condensation pressure, and by assuming a straight cylindrical pore model [13, 14].

The Mercury Intrusion experiments were carried out on a Porosimeter 4000 apparatus by Carlo Erba Instruments. A contact angle of 141.3° was used. The cumulative pore volume of the macroporous glass (MaPG) represents the total volume of mercury taken up by this sample at the given pressure. The pore diameter was calculated by applying the Washburn equation and a cylindrical pore model [15].

The Small Angle X-ray Scattering (SAXS) measurements were performed using nickelfiltered Cu K_α radiation. Loose powder layers of a thickness of 0.5–1.5 mm were prepared and interradiated. About 120 points of the smeared relative scattering intensities in the region of the scattering vector h, $0.05/\text{nm} < h < 3/\text{nm}$, were recorded point by point using a Kratky camera. About 2500 impulses from the scattering of the sample, after background subtraction, were obtained at the position $h_{\max} = 3/\text{nm}$. The experimental intensities have a dynamic of 5 decimal powers after the application of the special collimation correction procedure described in [16].

The theory of chord length distribution (c.l.d.) was applied to interprete the measured SAXS curves of the meso- and macroporous materials. This theory is briefly explained in the following:

Whenever a geometric figure is intersected by straight lines, chord length distribution results. There exists a complete theory [17] which connects the pure geometric theory of c.l.d. with the SAXS experiment. The deciding structure function in this field is the second derivative of the correlation function of SAXS, $\gamma''(d)$. On one side this function can be obtained experimentally [$I(h) \Rightarrow \gamma(d) \Rightarrow \gamma''(d)$, where $I(h) =$ isotropic scattering curve, $d =$ distance in nm] and on the other, it can be compared with models of stochastic geometry.

Pure geometric models for structure functions, like the three-dimensional correlation function (γ), for particle characterisation in the nm-region via SAXS are indispensable [17].

If the sequence of the chord segments on a straight line is totally irregular:

$$\begin{aligned}\gamma'' = \frac{1}{l\cdot(l-c)}[&\phi(l) + f(m) - 2\delta(0) + u_{21}(l+m+l)\\ &+ u_{12}(m+l+m) - 2u_{11}(l+m)\\ &- 2u_{22}(l+m+l+m) - \cdots] \end{aligned} \quad (1)$$

Equation 1 holds.

Here $\bar{l}$ is the mean chord length within the particle phase,

c is the porosity,

$\varphi(l)$ is the c.l.d. of the particle phase,

$f(m)$ is the c.l.d. within the space between the particles (pores),

$\delta(0)$ is the DIRAC-delta function,

the functions u_{ij} represent the sums of the chord segments.

Correlation functions result directly from the isotropic SAXS experiment, $I(h)$ [18]. Sample values of $I(h)$, $h = 4\pi/\lambda_0 \cdot \sin(\theta)$ (where $2\theta =$ scattering angle, $\lambda_0 =$ wavelength of the radiation used), can be completely led back to $\gamma(x)$ by Equation 2.

$$I(h) = \frac{\displaystyle\int_0^L 4\pi x^2 \cdot \gamma(x) \cdot \frac{\sin(h\cdot x)}{h\cdot x} \cdot \mathrm{d}x}{\displaystyle\int_0^L 4\pi x^2 \cdot \gamma(x) \cdot \mathrm{d}x}, \quad I(0) = 1 \quad (2)$$

In Equation 2 we used x instead of d. Generally, the inverse problem (determination of $\gamma(d)$ from $I(h)$ via the inverse transformation of Equation 2, which is an ill-posed problem), can be solved with an exactness which allows a comparison of experimental $\gamma(d)$ functions with theoretical ones, based on different geometric models, is appropriate. In this light, $\gamma(d)$ contains all the information that can be obtained from the scattering experiment, see Feigin and Svergun [18] and Guinier and Fournet [19].

Thus, considering the signs of the terms in Equation 1, the c.l.d.'s of the mesoporous "Two-Phase Porous Silica" and the macroporous glass in the range between 0 and 40 nm reflect the frequency of chord segments of length $l, m, l+m, l+m+l, m+l+m \ldots$. in the investigated sample.

Solid state ^{27}Al MAS NMR spectra were recorded on a Bruker AMX 400 spectrometer at 104.2 MHz.

The acidic properties of the aluminium modified mesoporous glasses were characterized using Temperature-Programmed Desorption (TPD) of ammonia. First, about 100 mg of each sample was activated in vacuum at 300°C. Then ammonia (purity 3.8, Messer-Griesheim) was adsorbed at 100°C and an equilibrium pressure of 18 kPa. The physisorbed ammonia was removed by isothermal evacuation. The loaded samples were evacuated in a quartz glass cuvette from 100 to 600°C with a heating rate of 5 K/min. The desorbed ammonia was detected with a mass spectrometer QTMD Carlo Erba Instruments.

3. Results

The porosity by nitrogen adsorption of the porous glasses prepared by various acid leaching conditions of the phase-separated sodium borosilicate initial glass is shown in Fig. 2. Shorter leaching time results in a microporous glass (MePG 1). According to the IUPAC-classification [20] the isotherm is of Type I without a hysteresis loop. Longer leaching times of the initial glass lead to mesoporous samples (MePG 2 and MePG 4). Both increasing concentration of the leaching solution from 3 to 6 N (MePG 3) and changing the leaching solution from HCl to $Al(NO_3)_3$ (MePG 5/1.0 and MePG 6/0.7), in combination with longer leaching times, also result in mesoporous materials. All isotherms are of Type IV with H1 (Fig. 2D) and H2 (Fig. 2B and C) hysteresis loops [20], a characteristic for total mesopore filling.

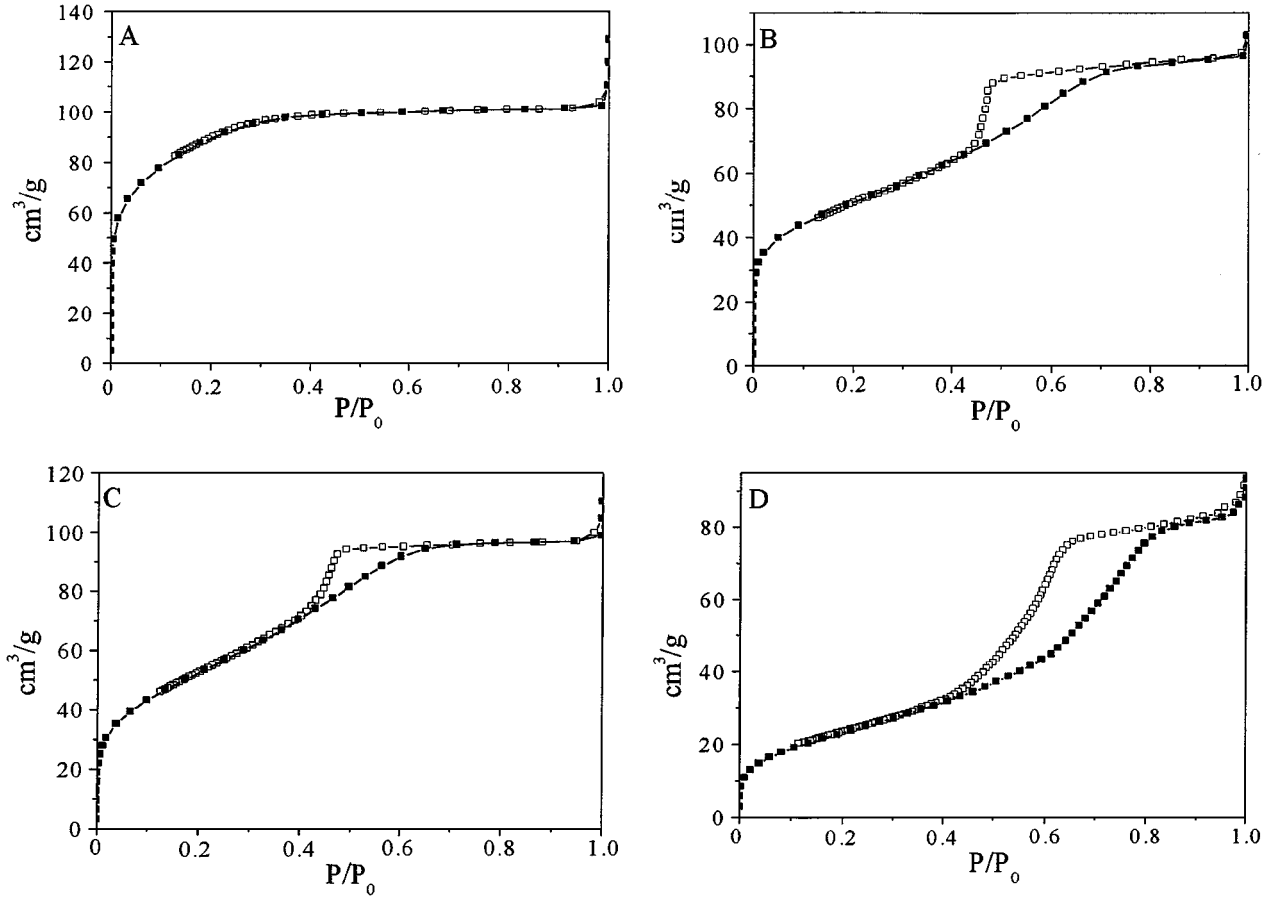

Figure 2 N_2 sorption isotherms of MePG 1 (A), MePG 2 (B), MePG 6/0.7 (C) and MePG 4 (D).

These trends are also illustrated in the textural properties of the porous glasses, obtained from these isotherms (Table II). The calculated surface areas vary between 337 m^2/g for the microporous glass MePG 1 and 86 m^2/g for the mesoporous glass MePG 4 prepared by long leaching times. The total pore volumes are relatively similar (0.14 to 0.18 cm^3/g).

The adsorption isotherm analysis of the investigated "Two-Phase Porous Silica" with the BJH method [13, 14] gives information about the pore structure of these materials. The pores can be assigned as cavities between packed uniform spherical particles. Because of pore blocking effects the desorption branch of the isotherms reflects the size distribution of the pore throats.

The differential pore size distributions of the "Two-Phase Porous Silica" given by the adsorption isotherm analysis are shown in Fig. 3. Longer leaching times lead

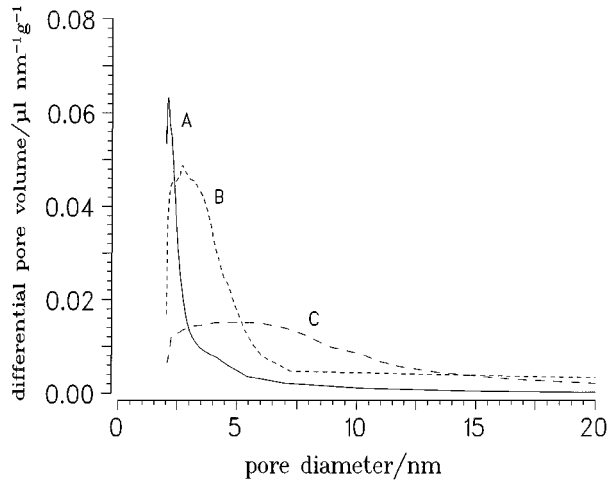

Figure 3 Pore size distributions of MePG 1 (A), MePG 6/0.7 (B) and MePG 4 (C) determined by adsorption isotherm analysis using the BJH method [13, 14].

TABLE II Texture properties of the porous glasses

sample	BET surface area [m^2/g]	pore volume [cm^3/g]	mean pore diameter[1)] [nm]	maximum pore diameter[1)] [nm]
MePG 1	337	0.185	2.7	2.1
MePG 2	183	0.158	4.3	2.9
MePG 3	181	0.169	4.1	2.8
MePG 4	86	0.136	6.6	3.5
MePG 5/1.0	188	0.156	3.4	2.8
MePG 6/0.7	196	0.180	3.5	2.7

[1)]adsorption isotherm analysis, BJH method [13, 14].

to an increase in pore sizes (Table II) and broader pore size distributions. Fig. 4 shows the pore size distribution of the mesoporous glass MePG 4 estimated from the desorption isotherm data, indicating the uniformity of the pore throats of this sample.

The macroporous "frame"-glass resulting from the conditions of phase-separation (630°C, 24 h) was formed after alkaline treatment of the mesoporous glass MePG 2. This procedure completely remove all the silica-gel phase from the macropores. The macroporous glass (MaPG) was characterized using Mercury

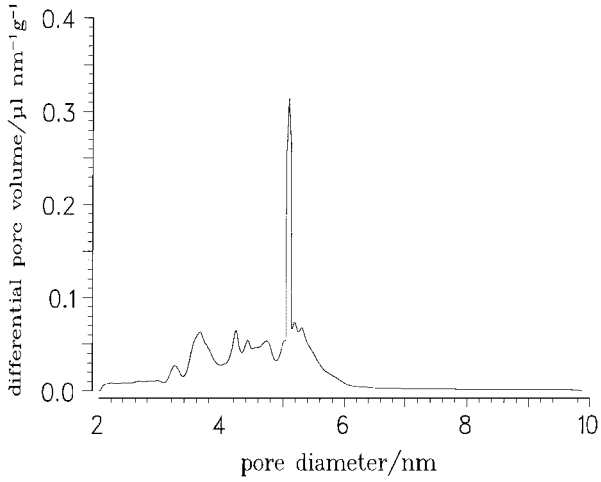

Figure 4 Pore size distribution of MePG 4 given by desorption isotherm analysis using the BJH method [13, 14].

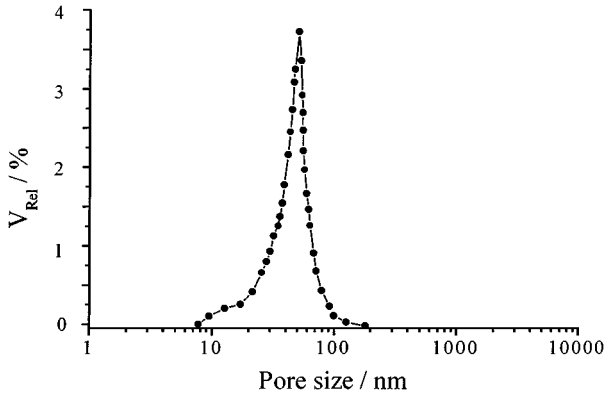

Figure 5 Pore size distribution of the "frame" glass (MaPG) determined by Mercury Intrusion.

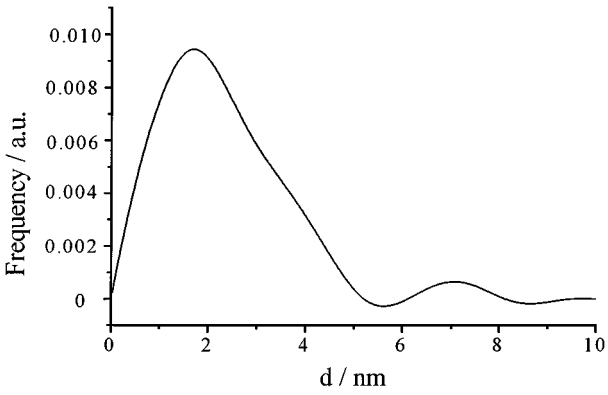

Figure 6 Chord length distribution ($\gamma''(d)$) for distances $d < 10$ nm of MePG 6/0.7.

Intrusion (Fig. 5). It possesses a specific surface area of 37 m^2/g, a total pore volume of about 0.493 cm^3/g and uniform pores with a mean diameter of 54 nm.

The local structures of the meso- and macroporous glasses were investigated by SAXS using the theory of chord length distribution (c.l.d.). The c.l.d. for distances $d < 10$ nm of the mesoporous glass MePG 6/0.7 is presented in Fig. 6. The sample shows a main maximum at about 2.0 nm. Additionally the c.l.d. is characterized by a shoulder near 4 nm and a maximum of lower intensity in the range between 7.0 and 7.5 nm. The c.l.d.'s

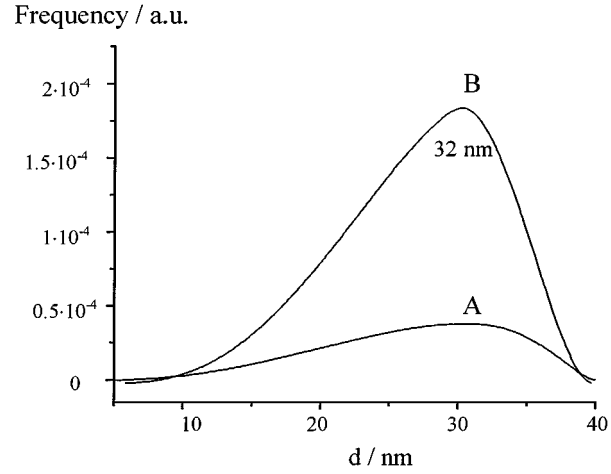

Figure 7 Chord length distributions ($\gamma''(d)$) of MePG 6/0.7 (A) and MaPG (B) in the range between 10 and 40 nm.

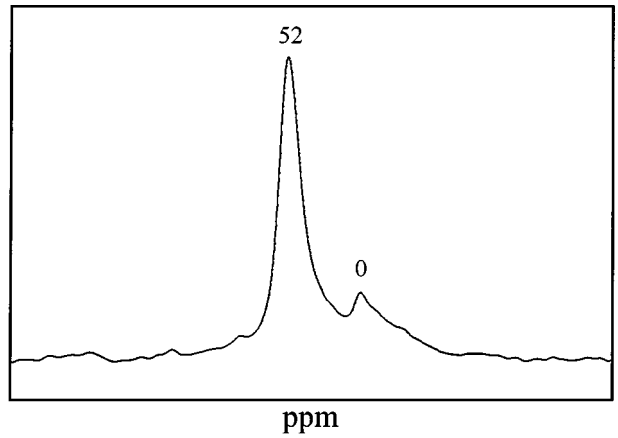

Figure 8 ^{27}Al MAS NMR spectrum of MePG 5/1.0.

of a mesoporous glass (MePG 6/0.7) and the macroporous glass (MaPG) in the d-range between 10 and 40 nm are shown in Fig. 7. The c.l.d.'s are of comparable form, for both porous glasses a maximum at about 32 nm is found. Differences exist in the intensities of the maxima. In the case of the mesoporous glass the lower intensity indicates that chord lengths of about 30 nm are not so frequent.

In addition to the general preparation procedure an aluminium modification of these "Two-Phase Porous Silica" can be achieved by a direct leaching with an Al-containing acid solution ($Al(NO_3)_3$-solution) followed by a subsequent calcination (samples MePG 5/1.0, MePG 6/0.7). This treatment greatly affects the surface acidity and catalytic properties of porous glasses [21]. Brönsted acid sites are formed by incorporation of aluminium in the silica-framework, aluminium places itself in tetrahedral coordination. For that reason it is important to establish the coordination state of aluminium in the modified mesoporous "Two-Phase Porous Silica" glasses. ^{27}Al MAS NMR measurements of the aluminium-containing mesoporous glass MePG 5/1.0 (Fig. 8) show that most aluminium are in tetrahedral coordination at 52 ppm. Only a small amount of aluminium is in the octahedral coordination at 0 ppm.

However, it cannot be decided yet whether the incorporation takes place in the mother glass phase of the

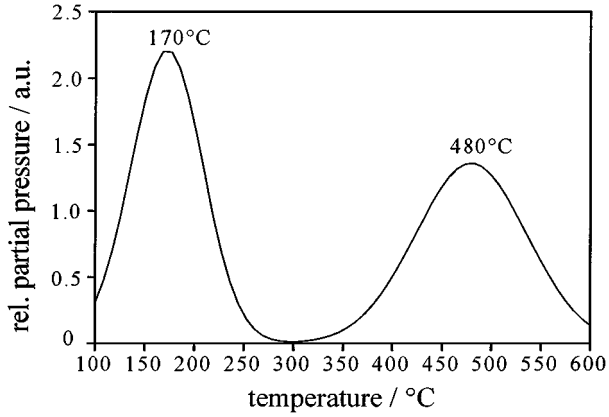

Figure 9 NH_3 TPD spectrum of MePG 5/1.0.

"frame"-CPG or in the finely dispersed silica-gel phase found inside the macropores.

The influence of aluminium modification on the acidic properties of the mesoporous "Two-Phase Porous Silica" is shown in the temperature programmed desorption spectrum of ammonia of the sample MePG 5/1.0 (Fig. 9). In comparison to other amorphous aluminosilicates the spectrum is remarkably good resolved. Two completely separated and nearly symmetrical peaks at 170°C and 480°C respectively are obtained.

The temperature of the peak maxima relates to the strength of the acid sites. The low temperature peak at 170°C is caused by ammonia species adsorbed on weak acid sites like the silanol or boranol groups. The peak at higher temperature results from the decomposition of ammonium ions and can be assigned to strong Brönsted acid sites.

4. Discussion

The existence of dissolved silica in the alkali-rich borate phase of the phase-separated alkali-borosilicate glass represents the first precondition to prepare "Two-Phase Porous Silica." The solubility of silica in the alkali-rich borate phase results from the asymmetry in the decomposition of glasses in the Na_2O-B_2O_3-SiO_2 system and can be assigned as secondary phase separation [7, 9]. The amount of silica dissolved in the soluble phase, is strongly controlled by the composition of the initial glass (i), temperature (ii) and time (iii) of the phase separation process.

At an early stage of the leaching process the silica-containing alkali-rich borate phase is completely dissolved in the acidic solution. If the $Si(OH)_4$ concentration in the leaching solution is too high, the dissolved silica coagulates in the main silica framework of the Controlled Pore Glass as finely dispersed silica-gel [22]. With increasing silica concentration in the alkali-rich borate phase, another formation mechanism of the finely dispersed silica must be taken into account. In this case the silica forms an independent network in the alkali-rich borate phase. This network is not dissolved in the acidic solution and retains its microstructure after the leaching process [23].

This means, that questions about the formation mechanism and the filling degree of the macroporous glass skeleton with finely dispersed silica can only be answered in combination with the properties of the phase-separated initial glass (composition, time and temperature of the heat treatment).

As a result of the formation mechanism the finely dispersed silica can be assigned as silica-xerogel. Therefore, in the case of completely dissolution of the silica in the leaching solution the structural and textural properties of the "Two-Phase Porous Silica" are influenced by the pH-value of the leaching solution, time and temperature of the leaching process and the type of leaching solution. In the case of an independent silica network in the soluble phase the microstructure parameters are predetermined and only special parameters (pore size, pore shape, specific surface area) can be varied through leaching conditions.

Our experimental results confirm the complete dissolution of the silica in the leaching solution during the preparation process of the "Two-Phase Porous Silica". The composition of the initial glass (B_2O_3/Na_2O molar ratio of 3) and the conditions of the heat-treatment lead to a high concentration of silica in the alkali-rich borate phase. The very low pH (<1) of the leaching solution forms a microporous silica-gel inside the original pores of the macroporous glass (MePG 1).

As for typical silica gels, the microstructure of the finely dispersed silica phase inside the macropores is formed by agglomeration of primary and secondary particles [24]. The pores are the cavities between the packed particles.

The structural and textural properties of microporous silica-gels can be modified by an acid treatment [25]. In dependence on the time of the treatment the micropore volume and size decreases. Concurrently mesopores are formed. The total pore volume remains constant. Modifications in the microstructure result from the dissolution of silica at the walls of larger pores and deposition in smaller ones [25, 26]. Same effects are obtained by longer leaching times of the phase-separated initial glass (Figs 2 and 3).

The above discussed microstructure parameters of the finely dispersed silica-gel phase can be investigated more in detail by comparative analysis of the results of nitrogen adsorption and SAXS. The pore size and chord length distributions of two mesoporous glasses are shown in Fig. 10.

For both samples a clear relationship between the pore size distributions determined through N_2 adsorption isotherm analysis and the c.l.d.'s is obtained. In both cases MePG 6/0.7 (A) shows a maximum between 2 and 3 nm and a shoulder at 3.5–4 nm, reflecting the mesopores. Above 6 nm the curves are different. The pore size distribution reveals no pores with diameters above 6 nm. Accordingly, in agreement with Barby's model of silica morphology [27] and Vengange [28] the maximum in the c.l.d. at 7.2 nm can be attributed to the mean diameter of the secondary particles of the finely dispersed silica-gel phase. The lower intensity of this maximum arises from smaller electron density fluctations between the secondary particles and the porous glass framework. The nearly symmetrical maxima in the c.l.d. indicate the high regularity in the sizes of mesopores and secondary particles.

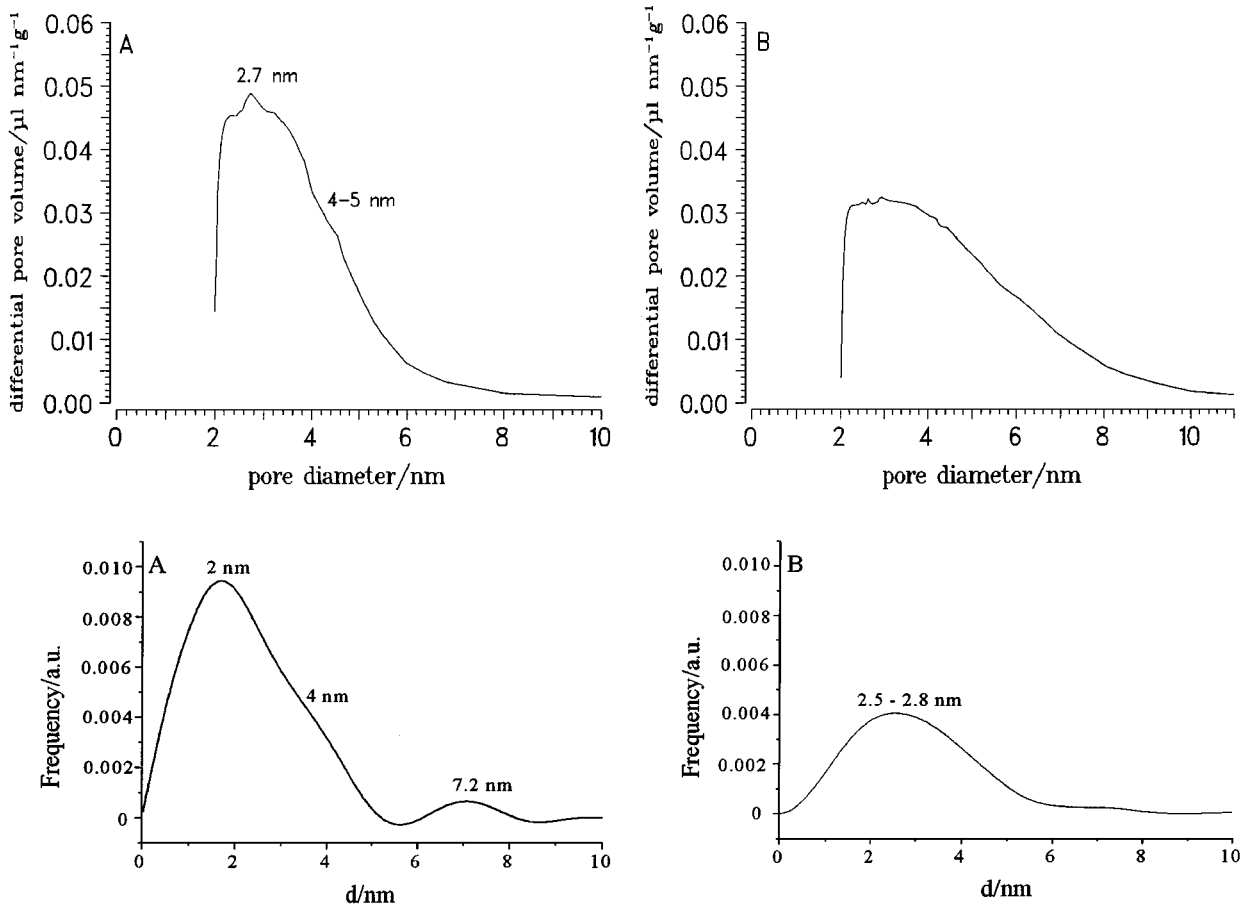

Figure 10 Pore size distributions given by adsorption isotherm analysis and chord length distributions for distances $d < 10$ nm of MePG 6/0.7 (A) and MePG 2 (B).

For MePG 2 (B) as well only one maximum of lower intensity is found in the pore size distribution as also in the c.l.d. The broader distributions of pore sizes and chord lengths resulting from the more disordered microstructure of this sample do not allow to obtain precise informations about structural and textural parameters. Nevertheless, resulting from the accordance with the pore size distribution the peak with a maximum at about 3 nm in the c.l.d. can be assigned to the mesopores.

The finely dispersed silica-gel almost completely fills the macropores of the Controlled Pore Glass. As a result the intensity of the maximum in the c.l.d. of the mesoporous glass (Fig. 7A) at about 32 nm is reduced. The complete filling of the macropores with finely dispersed silica-gel was also established by scanning electron microscopy and mercury intrusion [29] and follows from the optimal ratio of initial glass composition, conditions of heat-treatment and resulting macropore size. Only a small amount of the finely dispersed silica-gel on the outer surface of the glass spheres was removed during the acid leaching process.

Based on geometric models the estimation of the mean diameter of the macropores from the maxima in the c.l.d.'s in Fig. 7 requires the application of a conversion factor [30]. The applied conversion factor of 1.5 considers the curvature and finite nature of a real macropore in contrast to an infinitely long circular cylinder. In this case the mean chord length corresponds to the cylinder diameter. The conversion factor is 1. As well for the macroporous glass as for the mesoporous sample the applied conversion factor leads to a mean macropore diameter of

$$D = 32 \text{ nm} \cdot 1.5 = 48 \text{ nm} \quad (3)$$

which is in fair agreement with the results of the Mercury Intrusion experiments (Fig. 5).

Leaching of the phase-separated initial glass with an Al-containing acidic solution ($Al(NO_3)_3$) increases the surface acidity of the resulting "Two-Phase Porous Silica". Caused by the leaching conditions (pH value, leaching time) the textural properties are comparable to the unmodified samples (Table II). During leaching and calcination small amounts of aluminium (<1 wt.% Al_2O_3) are incorporated into the silica-framework of the finely dispersed silica-gel phase or in the macroporous "frame" glass. The TPD spectrum (Fig. 9) shows that at the surface of the aluminium modified mesoporous glasses beside weak acid silanol and boranol groups, strong Brönsted acid sites are also present, formed by the incorporated aluminium atoms. The symmetrical shape and the temperature of the peak maximum (480°C) indicate that these sites are homogeneously distributed and are compared to a reference zeolite (HZSM-5) [31] of higher strength.

4.1. Structure Modelling

On the basis of the results of the adsorption measurements, the Mercury Intrusion and SAXS it is possible

to describe the finely dispersed silica-gel phase qualitatively and quantitatively and to develop a model of the microstructure of the investigated "Two-Phase Porous Silica". As example, the mesoporous glass MePG 2 is considered.

The treatment of the sample MePG 2 with alkaline solution removes the finely dispersed silica-gel phase from the "frame"-pores, producing the macroporous glass MaPG. Assuming that during the alkaline treatment no framework silica is dissolved the volume ratio of the finely dispersed silica-gel phase to the "frame" Controlled Pore Glass (V_{gel}/V_{glass}) can be calculated from the total pore volumes of the macroporous glass MaPG (V_1) and the mesoporous glass MePG 2 (V_2) (Equations 4–6). An identical frame density of the silica-gel phase and the Controlled Pore Glass of 2.2 g/cm^3 is assumed.

$$V_1 = \frac{V_{MaP}}{\rho \cdot V_{glass}} \tag{4}$$

$$V_2 = \frac{V_{MaP} - V_{gel}}{\rho \cdot V_{glass} + \rho \cdot V_{gel}} \tag{5}$$

Here V_{MaP} is the volume of the macropores. Combination of Equations 4 and 5 leads to:

$$\begin{aligned} \frac{V_{gel}}{V_{glass}} &= \frac{\rho \cdot (V_2 - V_1)}{(-V_2 \cdot \rho - 1)} \\ &= \frac{2.2\,\text{g/cm}^3 \cdot (0.158\,\text{cm}^3/\text{g} - 0.493\,\text{cm}^3/\text{g})}{(-0.158\,\text{cm}^3/\text{g} \cdot 2.2\,\text{g/cm}^3 - 1)} \\ &= 0.547 \end{aligned} \tag{6}$$

Resulting from the identical frame densities the same mass ratio m_{gel}/m_{glass} is found. Now, the mass percentage of the finely dispersed silica gel phase can be calculated (Equation 7):

$$\begin{aligned} \frac{m_{gel}}{m_{glass}} &= 0.547 \\ m_{gel} + m_{glass} &= 100\,\text{wt.\%} \\ m_{gel} &= 35.4\,\text{wt.\%}. \end{aligned} \tag{7}$$

The mesoporous glass MePG 2 contains 35.4 wt.% finely dispersed silica-gel. For that reason on the basis of the textural properties of this sample (Table II) the finely dispersed silica-gel phase can be considered as a mesoporous silica-gel with a BET surface area of 573 m^2/g and a pore volume of about 0.446 cm^3/g. These values are in remarkably good agreement with the textural properties of an acid modified microporous silica-gel. After treatment with 3 N hydrochloric acid at 90°C for 6 hours the gel possesses mesopores in the range between 2 and 6 nm, a BET surface area of 586 m^2/g and a total pore volume of about 0.445 cm^3/g. The "external" surface of the silica-gel phase in the macropores is not freely accessible for the nitrogen molecules. This leads to the slightly lower BET surface area compared to the ordinary silica-gel. Fig. 11 shows the model of the mesoporous finely dispersed silica-gel in a single macropore of the Controlled Pore Glass (MaPG) based on the discussed experimental results.

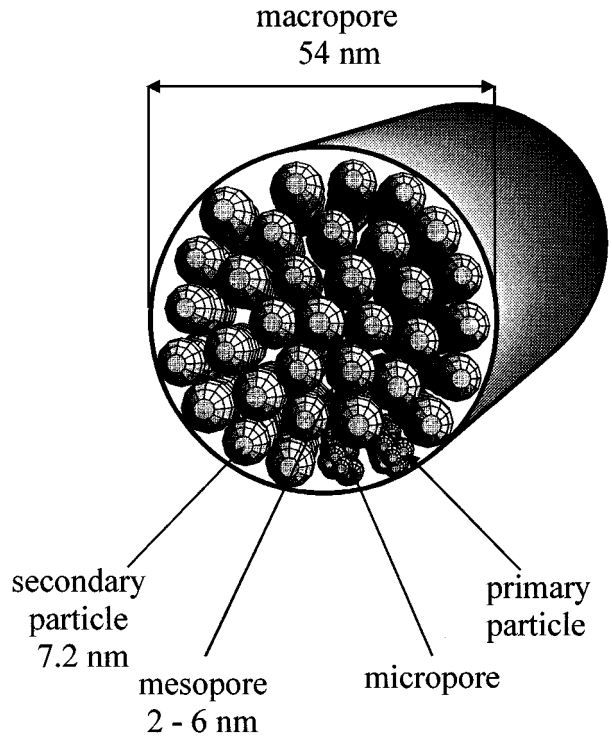

Figure 11 Model of the finely dispersed silica-gel in a single macropore.

5. Conclusions

This paper reports investigations of "Two-Phase Porous Silica" based on finely dispersed silica in the nearly completely filled macroporous cavities of the main silica framework of a Controlled Pore Glass. The finely dispersed silica can be assigned as acid treated silica-gel. Therefore, the type of porosity of the mesoporous glasses is related to the leaching treatment of the phase-separated sodium borosilicate initial glass. The acidic leaching conditions affect changes in pore structure of the silica-gel phase by dissolution and deposition processes of silica.

Application of various investigation methods (adsorption measurements, Mercury Intrusion, SAXS) allows a very detailled characterization of the microstructure of the amorphous "Two-Phase Porous Silica", particulary the size of individual structural parameters (pores, particles). From modelling results a better understanding of the microstructure of Controlled Pore Glasses based on SiO_2-rich sodium borosilicate initial glasses.

The surface acidity of the MePG can be changed by leaching with an Al-containing acidic solution. As a result strong Brönsted acid sites are formed. The Al-modified mesoporous glasses show comparable textural properties to the aluminium-free samples.

Possible applications of the mesoporous glass beads can be as catalyst for reactions of bulky organic compounds, as catalyst support or as packing material for HPLC. Recently, ultrathin porous glass membranes based on the discussed "Two-Phase Porous Silica" were developed. Such flat membranes possess a comparable

microstructure to the investigated glass beads [32]. The thin glass plates represent very interesting potential materials for use in gas separation, in the science of confined matter or as catalytic active membranes in microreaction engineering.

Another interesting field of research is the use of the finely dispersed silica-gel phase in the macropores as SiO_2-source for the preparation of CPG/zeolite nanocomposites.

References

1. T. TANAKA, A. GUILLEUX, T. OHYAMA, Y. Y. MARUO and T. HAYASHI, *Sensors and Actuators B* **56** (1999) 247.
2. K. KURAOKA, Z. SHUGEN, K. OKITA, T. KAKITANI and T. YAZAWA, *Journal of Membrane Science* **160** (1999) 31.
3. V. RESHETNYAK, L. SHANSKI, O. YAROSHCHUK, A. TERESHCHENKO, J. LINDAU, G. PELZL, F. JANOWSKI and K. OTTO, *Mol. Cryst. Liq. Cryst.* **329** (1999) 447.
4. F. JANOWSKI, G. FISCHER, W. URBANIAK, Z. FOLTYNOWICZ and B. MARCINIEC, *J. Chem. Tech. Biotechnol.* **51** (1991) 263.
5. R. LODKOWSKI, E. KRUSZYNSKA, Z. SUPRYNOWICZ and B. BUSZEWSKI, *Chem. Anal.* **39** (1994) 543.
6. US-Pat. 2.106.744 (1934), 2.215.039 (1940), 2.221.709 (1940).
7. F. JANOWSKI and W. HEYER "Poröse Gläser-Herstellung, Eigenschaften und Anwendung" (Deutscher Verlag für Grundstoffindustrie, Leipzig, 1982).
8. S. P. ZHDANOV, "The Structure of Glass" (Consultants Bureau, New York, 1958).
9. O. V. MAZURIN and G. P. ROSKOVA, in "Phase Separation in Glass," edited by O. V. Mazurin and E. A. Porai-Koshits (North-Holland, Amsterdam, 1984).
10. H. TANAKA, T. YAZAWA, K. EGUCHI, H. NAGASAWA, N. MATSUDA and T. EINISHI, *J. Non-Cryst. Solids* **65** (1984) 301.
11. W. HALLER, *J. Chem. Phys.* **42** (1965) 686.
12. S. BRUNAUER, P. H. EMMETT and E. TELLER, *J. Amer. Chem. Soc.* **60** (1938) 309.
13. E. P. BARRET, L. G. JOYNER and P. H. HALENDA, *ibid.* **73** (1951) 373.
14. P. A. WEBB and C. ORR, "Analytical Methods in Fine Particle Technology" (Micromeritics Instrument Corp., Norcross, 1997) p. 80.
15. E. W. WASHBURN, *Proc. Nat. Acad. Sci. U.S.A.* **7** (1921) 115.
16. W. GILLE, Ph.D. Thesis, Halle (Saale), 1983.
17. W. GILLE, D. ENKE and F. JANOWSKI, *Journal of Porous Materials*, in press; W. Gille, *Computational Materials Science* **18** (2000) 65.
18. L. A. FEIGIN and D. I. SVERGUN "Structure Analysis by Small-Angle X-Ray and Neutron Scattering" (Plenum Press, New York, 1987).
19. A. GUINIER and G. FOURNET "Small-Angle Scattering of X-Rays" (John Wiley & Sons, New York, 1955).
20. K. S. W. SING, D. H. EVERETT, R. A. W. HAUL, L. MOSCOU, R. PIEROTTI, J. ROUQUEROL and T. A. SIEMIENIEWSKA, *Pure Appl. Chem.* **57** (1985) 603.
21. F. JANOWSKI, D. SCHUBERT and F. WOLF, *React. Kinet. Catal. Lett.* **22** (1983) 19.
22. S. P. ZHDANOV, *Trudy Gos. Opt. Inst.* **24** (1956) 86.
23. D. P. DOBYCHIN, in Proc. II. All-Union Conf. on Glass Structure, St. Petersburg, 1953, p. 176.
24. R. K. ILER, "The Chemistry of Silica" (John Wiley & Sons, New York, 1979).
25. F. JANOWSKI and F. WOLF, *Z. anorg. allg. Chem.* **434** (1977) 297.
26. W. D. MACHIN and P. D. GOLDING, *Langmuir* **5** (1989) 608.
27. D. BARBY, in G. D. Parfitt and K. S. W. Sing (eds.) "Characterization of Powder Surfaces" (Academic Press, London, 1976) p. 353.
28. V. VENDANGE and PH. COLOMBAN, *J. Mater. Res.* **11** (1996) 518.
29. D. ENKE, W. GILLE, W. SCHWIEGER and F. JANOWSKI, *Colloids and Surfaces A*, submitted.
30. D. ENKE, F. JANOWSKI, W. HEYER, W. GILLE and W. SCHWIEGER, in "Applied Mineralogy in Research, Economy, Technology, Ecology and Culture," edited by D. Rammlmair, J. Mederer, T. Oberthür, R. B. Heimann and H. Pentinghaus (Balkema, Rotterdam, 2000) p. 135.
31. W. SCHWIEGER, *Z. Phys. Chem.* **271** (1990) 243.
32. K. OTTO, Dissertation Halle, 2000.

Received 20 October 1999
and accepted 8 November 2000